Computational Investigation of Thermal Decomposition Mechanism of 5-Nitro-5-R-1,3-Dioxane Compounds

Pablo Andrés Ruiz (paruizr@unal.edu.co)
Universidad Nacional de Colombia Sede Medellin https://orcid.org/0000-0002-7120-8904
Silvia Quijano
Universidad Santiago de Cali
Jairo Quijano
Universidad Nacional de Colombia Sede Medellin

Research Article

Keywords: bronidox, DFT, nitrous acid, substituted dioxanes, thermal decomposition, 5-Nitro-5-R-1,3-dioxanes

Posted Date: November 8th, 2021

DOI: https://doi.org/10.21203/rs.3.rs-1025219/v1

Abstract

This paper features the results of the computational study of thermal decomposition reaction of 5-nitro-5-R-1,3-dioxane compounds, with R=H, Br and CH_3. Computational calculations were performed on M06-2X/6-311+G(d,p) in gas phase and also in solution with DMSO, at different temperatures. The kinetic and thermodynamic data obtained indicate a favoring of the reaction when the molecule presents a CH_3 substituent group in position 5 and when carried out in DMSO, the stability of the molecules in their energetic components was discussed, too. For R=H two different reaction mechanisms were proposed and studied. Wiberg bonds indices were obtained for the reactions studied and the results were examined in terms of bond formation and bond breaking progress as well.

Introduction

Compounds of 1,3-dioxane type are involved in industrial processes as by-products, when used as solvents [1], or as reagents in synthesis processes in fine organic chemistry [2]. They have also been reported as biologically active compounds with anti-inflammatory properties, and effective modulators of multidrug resistance [3]. These compounds have also been considered for their enormous potential in terms of structural diversity, especially by substitution at positions 2 and 5 of the molecule [4, 5]. 1,3 substituted molecules were found to display significant antifungal and antibacterial properties. Within this family of compounds, the most prominent have been the nitro and halonitro derivatives, especially because of their stability at a wider pH range (5-9). For instance, 5-bromo-5-nitro-1,3-dioxane (bronidox) exhibits a broad spectrum of antimicrobial activity [5] and is an important reagent for ion-radical and oxide-reduction type reactions [2 - 6].

5-bromo-5-nitro-1,3-dioxane is used as a preservative in rinses, cosmetics and toiletries such as: make-up, perfumes, toothpastes, soaps, shampoos, hand creams, facial scrubs, etc. [7].

Compounds derived from 1,3-dioxane can thermally decompose and release nitrous acid (HNO_2) or nitrogen oxides (NOx) depending on the reaction mechanism [8, 9].

There is an experimental study of the thermal decomposition of 5-nitro-5-R-1,3-dioxane type compounds (Figure 1 represents their general structure), in which the authors proposed a thermal decomposition mechanism for nitrous acid formation, similarly as represented in Figure 2 [10].

Although there are computational studies on the formation of 1,3-dioxane compounds [11] we are not aware of published theoretical studies on their thermal decomposition.

The development of this project sought to computationally study the thermal decomposition of a series of 5-nitro-5-R-1,3-dioxane compounds at different temperatures. The findings obtained allowed to deepen in the reaction mechanism of their decomposition, to obtain the kinetic and thermodynamic parameters of the reaction as well as to correlate the reaction rate with the structural characteristics of the molecules studied.

Methods

All calculations for this study were carried out in the Gaussian 09 computational package [12]. The geometrical parameters for all reactants, transition states and products of the reaction studied were optimized using the density functional theory (DFT), with the functional M06-2X [13] and 6-311+G(d,P) basis set [14].

(Pre-calculations were performed on the molecules studied, but there were no significant differences in the results with larger basis set).

Vibrational frequency calculations were conducted to obtain the kinetic and thermodynamic parameters of the reactions, which also allowed to characterize each structure as a minimum or saddle point within the potential energy surface. A scaling factor of 0.9658 was used to correct the zero-point vibrational energy (ZPE), as previously recommended [15].

Computational calculations were accomplished at five different temperatures within the range of 503 - 563 K and 1 atm of pressure.

Enthalpies and entropies values were evaluated according to the standard thermodynamics equations [16]. Calculations in solution with dimethyl sulfoxide (DMSO) were achieved by the polarizable continuum model, using the integral equation formalism (IEFPCM) [17].

Calculations of the intrinsic reaction coordinate (IRC) [18] were performed on each of the localized transition state structures to verify that they connect to the corresponding stationary minimum points corresponding to the reactants and products.

The kinetic parameters were evaluated using classical transition state theory (TST) according to the Eyring-Polanyi equation [19, 20].

The population partitioning technique, Natural Bond Orbital (NBO) [21, 22], has been used using the NBO program [23] implemented in the Gaussian 09 computational package [12]. Bond characteristics were obtained through Wiberg bond indices [24]. They are interpreted as a measure of bond order and bond strength among atoms. Processing these values generates additional indicators of both the bonds and the reaction. The percentage of evolution (%EV) is an indicator of the relative variation of the bond in the transition state, and has been calculated as:

$\%EV = \delta\beta_i \times 100$ (1)

Where, $\delta\beta_i = (\beta_i^P - \beta_i^R)/(\beta_i^P - \beta_i^R)$ (2)

Another important indicator calculated is the average relative variation[25],

$\delta\beta av = 1/n \Sigma \delta\beta_i$ (3)

Where *n* is the number of bonds to be considered in the reaction. The value obtained allows inferring characteristics of the transition state and is interpreted as a measure of the degree of progress of the transition state along the reaction coordinate.

The reaction is characterized by absolute synchronicity [25] (Sy), calculated from the Wiberg bond indices, according to the following expression:

$$S_y = 1 - \left[\frac{1}{(2n-2)}\sum\frac{|\delta\beta_i - \delta\beta_{av}|}{\delta\beta_{av}}\right] \quad (4)$$

Sy is an indicator ranging from 0 to 1, high values for Sy imply that the reaction is highly synchronous.

Results And Discussion

Mechanism of the decomposition reaction

The thermal decomposition reaction of a series of 5-nitro-5-R-1,3-dioxane compounds with R= H, CH_3 and Br, was computationally modeled to observe the effect of the substituent group on the reaction parameters and mechanism.

The reactions were carried out under conditions simulating the gas phase and also in solution with DMSO as solvent. The mechanisms postulated in Figures 2 and 3 were used as a starting point

Figure 2 represents a reaction mechanism that proceeds through a 5-atom cyclic transition state and involves the breaking of the carbon-nitrogen bond and the migration of a hydrogen from carbon 6 to one of the oxygens of the nitro group, thus leading to the subsequent formation of the alkene: 5-R-4H-1,3-dioxine and a nitrous acid molecule.

Alternatively, when R=H, the two-stage mechanism depicted in Figure 3 was also followed, where the reaction starts with the breaking of the C4-O3 and N9-C5 bonds and the formation of new bonds between C6-O3 and C4-N9. This leads to the formation of the intermediate compound 4-(nitromethyl)-1,3-dioxolane, which in a later stage decomposes through a cyclic transition state of 5 atoms. This involves the migration of hydrogen from carbon 5 and the detachment of the nitro group. The alkene 4-methylene-1,3-dioxolane is also produced by the formation of double bonds at carbons 4 and 5.

Kinetic and thermodynamic parameters

Computational optimization of the molecules was accomplished at M06-2X/6-311+G(d,p) in the temperature range of 503.15 – 563.15 K. Figure 4 depict the optimized geometry of the reactants, transition states (TS1-5-H-M1, TS1-5-methyl-M1 and TS1-5-Br-M1) and products (P1-H, P1-methyl and P1-Br) involved in the decomposition reactions, following the one-stage mechanism.

The vibrational frequency data and the linearization of the Arrhenius equation allowed to calculate the kinetic values shown in Table 1. It is worth noticing that the lowest activation energies (Ea and $\Delta G^{\neq}$) for

the decomposition reaction are given in their order for the molecules with R = methyl, Br and H.

An important contribution to the decrease of the free energy of activation can be noticed in the activation entropy with the highest value 12.4 $J \bullet mol^{-1} \bullet K^{-1}$ for methyl as a substituent group, which is also evident when looking at the values of the frequency factor (A).

Table 1
Kinetic parameters obtained from computational modeling at 523 K, for thermal decomposition of the studied compounds according to the one-stage mechanism. First inlet gas phase, second inlet solution with DMSO

R	k (s^{-1})	k_{DMSO}/k_{gas}	Ea (kJ mol^{-1})	A (s^{-1})	$\Delta G^{\neq}$ (kJ mol^{-1})	$\Delta S^{\neq}$ (J mol^{-1} K^{-1})
H	4.06×10^{-8} (1.82×10^{-7})	4.5	212.1 (207.0)	6.14×10^{13} (8.59×10^{13})	204.6 (198.1)	5.9 (7.619)
H[a]	2.04×10^{-17}				297.7	13.752
H[b]	1.47×10^{-9}				219.0	-12.401
Methyl	4.19×10^{-7} (3.39×10^{-5})	80.9	205.3 (192.8)	1.33×10^{14} (6.09×10^{14})	194.4 (175.3)	12.4 (15.564)
Br	1.39×10^{-7} (2.21×10^{-7})	1.6	208.2 (207.2)	8.66×10^{13} (1.098×10^{14})	199.3 (197.2)	8.9 (7.686)

[a]Mechanism figure 3, stage 1, gas phase [b]Mechanism figure 3, stage 2, gas phase

The two-stage mechanism turned out not to be feasible for the decomposition reaction 5-nitro-1,3-dioxane compared to that occurring in a single-stage mechanism. We see that the first stage is the limiting of the speed with a free energy of activation of 297.7 $kJ \bullet mol^{-1}$, that is 93 $kJ \bullet mol^{-1}$ higher than the activation free energy in the reaction occurring according to the single-stage mechanism.

When the reactions are carried out in solution with DMSO, the energy barrier in each of them is lowered and as a result the decomposition rate increases. The most important solvent effect occurs in the decomposition reaction of 5-methyl-5-nitro-1,3-dioxane, where the reaction rate is increased by more than 80 times.

It is also observed that when the substituent is a bromine atom, solvent stabilization is practically nonexistent.

Figure 5 features the optimized structures involved in the reaction by the proposed two-stage mechanism. Table 2 summarizes the experimental values reported for the modeled decomposition reactions.

The computational findings obtained, present a great discordance with the experimental findings reported by Stepanov. et.al, 2011 [10]. On the one hand, the reaction rates obtained computationally in this work are lower than the rates reported experimentally and on the other hand, the results reported by the authors indicate that the greatest favorability for the decomposition reactions occurs with the bromine atom in position 5. Our results indicate greater favorability of the decomposition reaction with the methyl group as a substituent.

The free energy profile for the reaction in gas phase and in DMSO is shown in Figure 6.

Table 2
Experimental kinetic parameters reported [1] in gas phase for the decomposition reactions of the 5-R-5-nitro-1,3-dioxane compounds studied at 523 K

R	K (s^{-1}) x 10^{-4}	Ea (kJ mol^{-1})	Log A	$\Delta S^{\neq}$(J mol^{-1} K^{-1})
H	0.33	173.1	12.81	-12.7
Methyl	2.59	170.1	13.40	-1.4
Br	5.56	167.7	13.42	-1.0

From the graphical representation it can be observed that the decomposition reaction of 5-bromo-5-nitro-1,3-dioxane compounds generates the most stable products even though kinetically it is not the most favored reaction among the reactions observed. The reactions in DMSO solution occur with a lower activation free energy value, however, the thermodynamics of the reaction are not significantly favored.

The substituent group on carbon 5 favors the elimination reaction and this occurs more rapidly with the methyl group.

Population analysis (NBO)

The natural bond orbital (NBO) population partitioning technique was used to obtain the Wiberg bond index values and by means of them to follow in depth the processes of bond breaking and bond formation throughout the chemical reaction.

The findings obtained from the NBO analysis and the other indicators that were calculated with equations 1, 2, 3 and 4 are depicted in Table 3.

Table 3
Wiberg bond indices for reactants, transition states and products (B_i^R, B_i^{TS} and B_i^P) for gas-phase decomposition reactions using the one-stage mechanism. (1) R=H, (2) R=Me, (3) R=Br. %EV: percentage of evolution; δβav: average relative variation; Sy: absolute synchronicity of the reaction

	C_5-C_6	C_6-H_7	H_7-O_8	O_8-N_9	N_9-C_5
B_i^R (1)	0.9793	0.9217	0.0022	1.5178	0.8763
(2)	0.9633	0.9203	0.0025	1.5147	0.8451
(3)	0.9862	0.9083	0.0008	1.5339	0.8408
B_i^{TS} (1)	1.3882	0.4261	0.3176	1.372	0.278
(2)	1.3524	0.4393	0.3006	1.3743	0.1187
(3)	1.3527	0.4249	0.3183	1.371	0.2694
B_i^P (1)	1.8559	0.0000	0.752	1.0947	0.0000
(2)	1.8092	0.0000	0.752	1.0947	0.0000
(3)	1.795	0.0000	0.752	1.0947	0.0000
%EV (1)	46.65	53.77	42.06	34.46	68.28
(2)	46.00	52.27	39.77	33.43	85.95
(3)	45.31	53.22	42.27	37.09	67.96
		δβav =	(1) 0.49	Sy =	(1) 0.88
			(2) 0.51		(2) 0.83
			(3) 0.49		(3) 0.88

The %EV shows us that in the transition state the C-N bond breaking processes are quite advanced processes for the decomposition reactions. We could relate this to an increase in the degrees of freedom of the structure representing the transition state and consequently a higher entropy, which fits the kinetic data reported in Table 1.

The methyl substituent at position 5 stabilizes the same carbon, perhaps due to its ability to induce electrons, which is why the C-N bond breaking process is the most advanced, approximately 86% compared to 68 % for the H and Br atoms. The substituent at C5 delays the alkene formation and slightly delays oxygen migration as well.

Bromine as a substituent, likely due to its electron-scattering effect, decreases the availability of carbon-carbon double bond formation and increases the advance of O-H and N-O bond formation perhaps due to

chain effects on the hydrogen electron cloud.

The average relative variation of the bond indices, δβav, with values of 0.49 and 0.51 for the reactions, indicates symmetric transitions states whose structure is intermediate between reactants and products.

The reaction that occurs for the molecule with the methyl substituent presents an imbalance between bond formation and bond breaking events, evidenced by a value of 0.83 for the reaction synchronicity.

Conclusions

Two possible reaction mechanisms for the thermal decomposition of 5-nitro-1,3-dioxane were considered. The findings of the computational calculations indicate that the two-stage mechanism for this reaction is not feasible with respect to the single-stage mechanism. When this compound is substituted at the carbon 5 position by a methyl group or a bromine atom the rate of the reaction becomes higher, mainly with the methyl group, and if the reaction is also carried out in solution with a solvent such as DMSO, the rate constant becomes approximately 80 times higher with respect to the reaction in the gas phase.

The values of kinetic and thermodynamic parameters obtained in this study and through the density functional theory, depart from the experimental values previously reported by Stepanov, et. al. 2011 [10].

The analysis of the Wiberg bond indices for the reaction studied allowed us to define carbon-nitrogen and nitrogen-oxygen bond breaking as the most and least advanced processes in each of the reactions, respectively.

Declarations

Acknowledgements

The authors are grateful for the support received by Universidad Nacional de Colombia – Medellin Headquarters during the research and publication stages of this work. S.Q also thanks to Dirección General de Investigaciones of Universidad Santiago de Cali (DGI), Santiago de Cali. P.R also thanks Instituto Tecnológico Metropolitano (ITM).

Statements and Declarations

Funding No funds, grants, or other support was received.

Competing Interests The authors declare that they have no conflict of interest.

Availability of data and material The datasets generated during and/or analysed during the current study are available from the corresponding author on reasonable request.

Code availability Not applicable

Authors' contributions The contribution of each author listed is based on: Silvia Quijano and Pablo Ruiz, made a substantial contribution to conception and design, data acquisition and analysis and interpretation of data; Pablo Ruiz and Jairo Quijano drafted the article and critically reviewed the intellectual content**.** All authors read and approved the final manuscript.

References

1. Carrera G, Vegué L, Boleda MR, and Ventura F (2017) Simultaneous determination of the potential carcinogen 1,4-dioxane and malodorous alkyl-1,3-dioxanes and alkyl-1,3-dioxolanes in environmental waters by solid-phase extraction and gas chromatography tandem mass spectrometry. J Chromatogr A 1487: 1–13
2. Kuramshina AE, Kuznetsov VV (2010) Quantum-chemical study of 1,3-dioxane complexes with two water molecules. Russ J Org Chem 46: 665–669
3. Zeng L, Xu G, Gao P, Zhang M, Li H, Zhang J (2015) Design, synthesis and evaluation of a novel class of glucosamine mimetic peptides containing 1,3-dioxane. Eur J Med Chem 93: 109–120
4. Wong JC, Sternson SM, Louca JB, Hong R, Schreiber SL (2004) Modular synthesis and preliminary biological evaluation of stereochemically diverse 1,3-dioxanes. Chem Biol 11: 1279–1291
5. Lapass LC, Hirsch CA, Winely CL (1976) Substituted 5-nitro-1,3 -dioxanes: correlation of chemical structure and antimicrobial activity. J Pharm Sci 65: 1301–1305
6. Adelaide T, Adebayo W, Rusell B, Salt WG (1987) Radical-nucleophilic Substitution (SRN1) Reactions. Part 5. Anions of nitroimidazoles in SRN1 and oxidative addition reactions. J Chem Soc Perkin Trans I 2819–2827
7. Fernandez-Alvarez M, Lamas JP, Sanchez-Prado L, Llompart M, Garcia-Jares C, Lores M (2010) Development of a solid-phase microextraction gas chromatography with microelectron-capture detection method for the determination of 5-bromo-5-nitro-1,3-dioxane in rinse-off cosmetics. J Chromatogr A 1217: 6634–6639
8. Stepanov RS, Kruglyakova LA, Astakhov AM, Golubtsova OA (2004) Kinetics and mechanism of thermal decomposition of 2-substituted 5,5-dinitro-1,3-dioxanes. Russ J Gen Chem 74: 1579–1582
9. Lytko-Krasuska A, Piotrowska H, Urbanski T (1979) Reductive elimination of a tertiary nitro group in 5-nitro- 1,3-dioxanes. Tetrahedron Lett 20: 1243–1246
10. Stepanov RS, Kruglyakova LA, Golubtsova OA (2011) Kinetics of thermolysis of 5-nitro-5-R-1,3-dioxanes. Russ J Gen Chem 81: 151–152
11. Kupova OY, Vakulin IV, Talipov RF (2013) Ab initio study of 1,3-dioxanes formation from formaldehyde dimer and alkenes. Comput Theor Chem 1013: 57–61
12. Frisch MJ, Trucks GW, Schlegel HB, Scuseria GE, Robb MA, Cheeseman JR, Scalmani G, Barone V, Mennucci B, Petersson GA, Nakatsuji H, Caricato M, Li X, Hratchian HP, Izmaylov AF, Bloino J, Zheng G, Sonnenberg JL, Hada M, Ehara M, Toyota K, Fukuda R, Hasegawa J, Ishida M, Nakajima T, Honda Y, Kitao O, Nakai H, Vreven T, Montgomery Jr JA, Peralta JE, Ogliaro F, Bearpark M, Heyd JJ, Brothers

E, Kudin KN, Staroverov VN, Kobayashi R, Normand J, Raghavachari K, Rendell A, Burant JC, Iyengar SS, Tomasi J, Cossi M, Rega N, Millam JM, Klene M, Knox JE, Cross JB, Bakken V, Adamo C, Jaramillo J, Gomperts R, Stratmann RE, Yazyev O, Austin AJ, Cammi R, Pomelli C, Ochterski JW, Martin RL, Morokuma K, Zakrzewski VG, Voth GA, Salvador P, Dannenberg JJ, Dapprich S, Daniels AD, Farkas O, Foresman JB, Ortiz JV, Cioslowski J, Fox DJ (2010) Gaussian 09, Revision B.01, Gaussian Inc., Wallingford CT

13. Zhao Y, Truhlar DG (2008) The M06 suite of density functionals for main group thermochemistry, thermochemical kinetics, noncovalent interactions, excited states, and transition elements: Two new functionals and systematic testing of four M06-class functionals and 12 other function. Theor Chem Acc 120: 215–241
14. Ditchfield R, Hehre WJ, Pople JA (1971) Self-consistent molecular-orbital methods. IX. An extended gaussian-type basis for molecular-orbital studies of organic molecules. J Chem Phys 54: 724–728
15. Merrick JP, Moran D, Radom L (2007) An evaluation of harmonic vibrational frequency scale factors. J Phys Chem A 111: 11683–11700
16. McQuarrie DA, Simon JD (1999) Molecular Thermodynamics. University Science Books, Sausalito, CA
17. Tomasi J, Mennucci B, Cammi R (2005) Quantum mechanical continuum solvation models. Chem Rev 105: 2999–3094
18. Fukui, K (1970) A formulation of the reaction coordinate. J Phys Chem 74: 4161–4163
19. Glasstone S, Laidler K, Eyring H (1941) In: The Theory of Rate Processes, 1st edn. McGraw Hill, New York
20. Benson SW (1969) the Foundations of Chemical Kinetics. McGraw-Hill, New York
21. Reed AE, Weinhold FJ (1983) Natural bond orbital analysis of near-Hartree–Fock water dimer. Chem Phys 78: 4066–4073
22. Reed AE, Curtiss LA, Weinhold F (1988) Intermolecular interactions from a natural bond orbital, donor-acceptor viewpoint. Chem Rev 88: 899–926
23. Glendening ED, Reed AE, Carpenter JE, Weinhold F (1988) NBO Version 3.1. Madison WI
24. Wiberg KB (1968) Application of the pople-santry-segal CNDO method to the cyclopropylcarbinyl and cyclobutyl cation and to bicyclobutane. Tetrahedron: 24: 1083–1096
25. Moyano A, Pericas MA, Valentí E (1989) A theoretical study on the mechanism of the thermal and the acid-catalyzed decarboxylation of 2-oxetanones (β-lactones). J Org Chem 54: 573–582

Figures

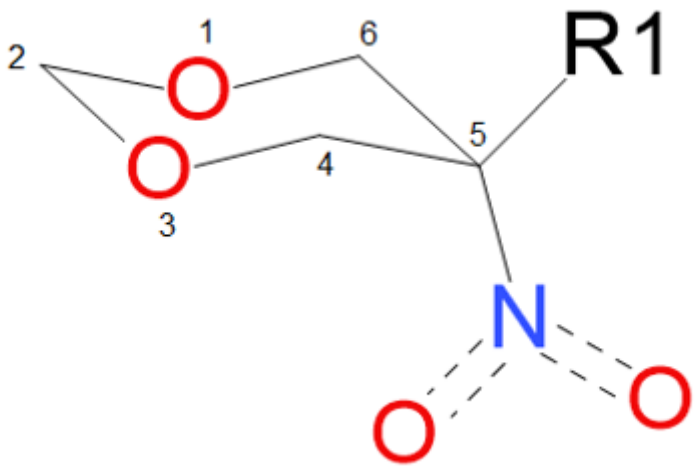

Figure 1

Structure representation of 5-nitro-5-R-1,3-dioxane compounds

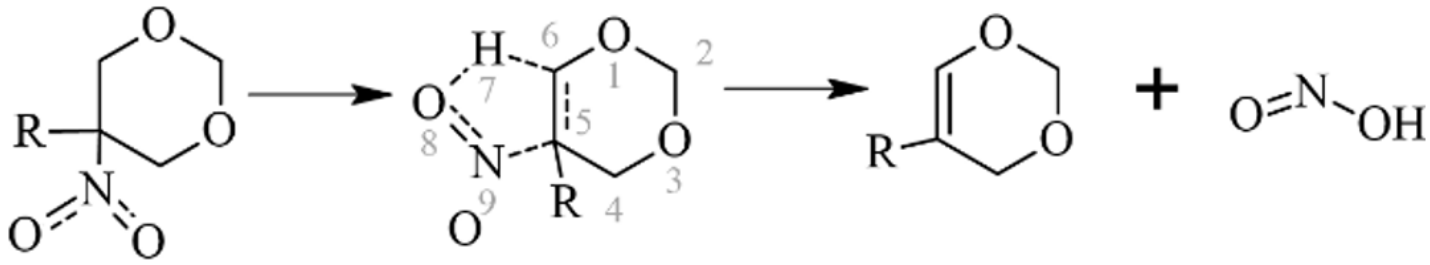

Figure 2

One-stage reaction mechanism of the thermal decomposition of 5-nitro-5-R-1,3-dioxanes, R= H, CH3, Br

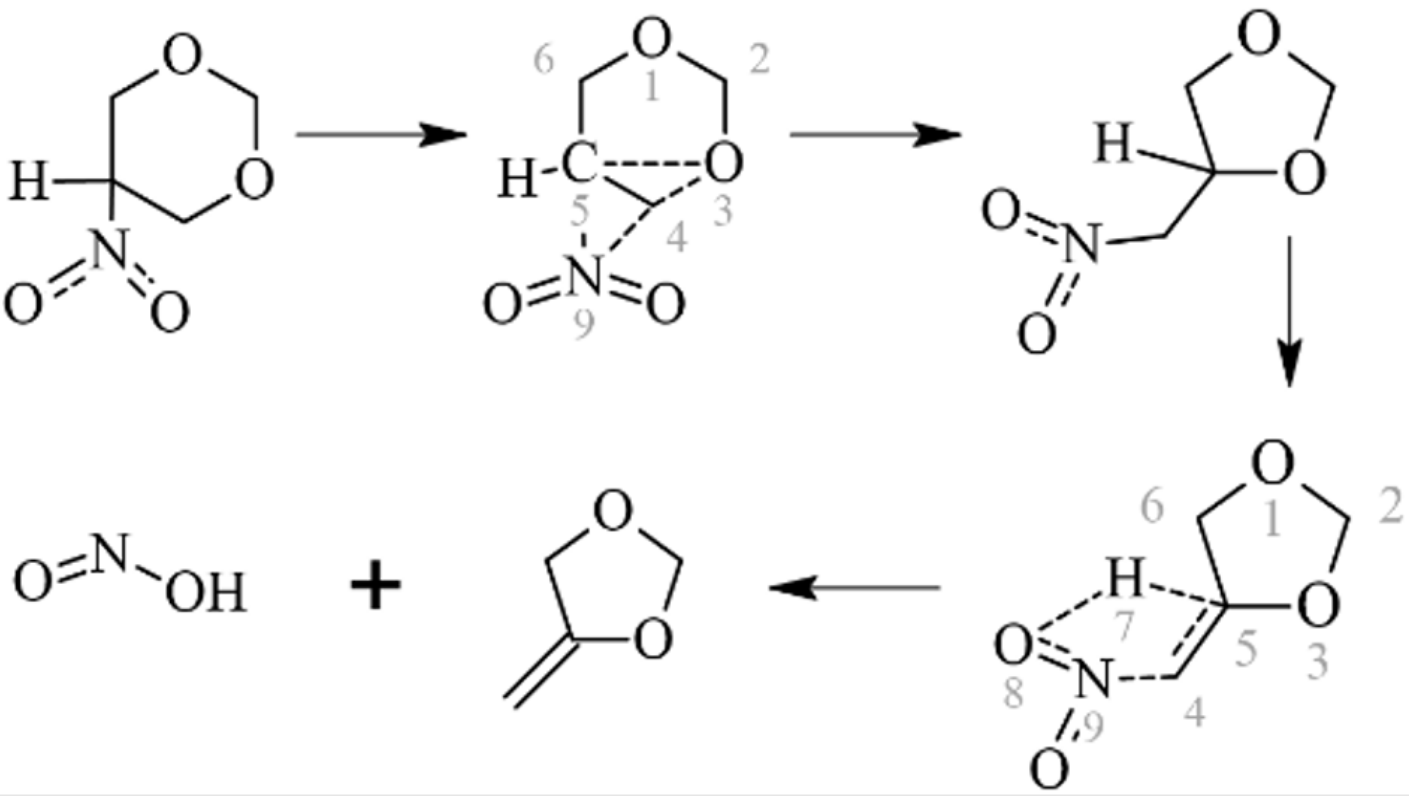

Figure 3

Two-stage mechanism, when the substituent at position 5 is R=H

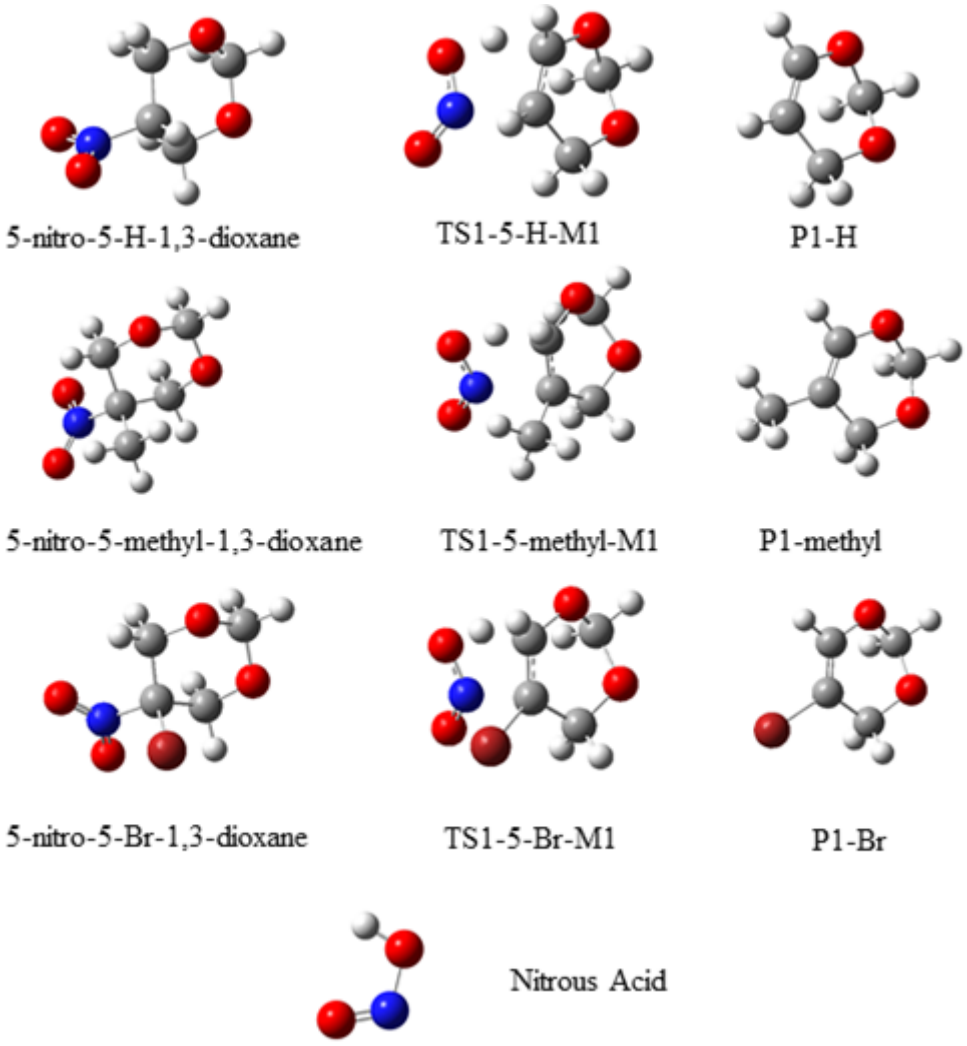

Figure 4

Molecules optimized for the structure involved in the decomposition reactions by the one-stage mechanism

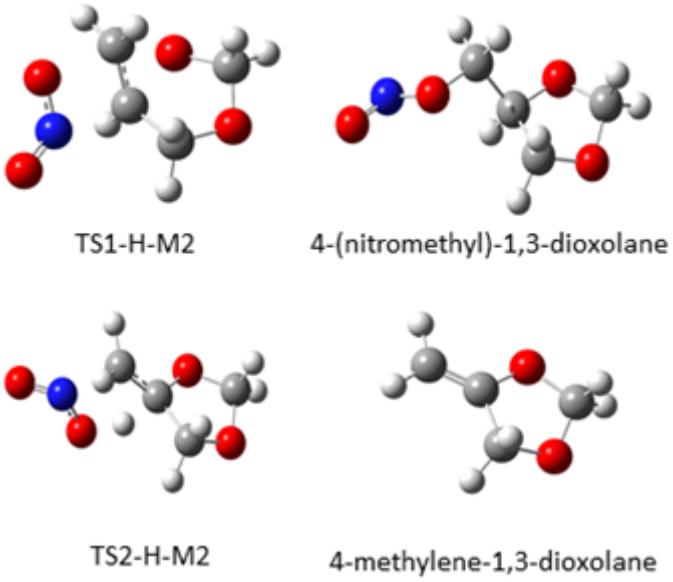

Figure 5

Gas-phase optimized molecules, according to the two-stage mechanism for R=H. Stage 1 transition state (TS1-H-M2), intermediate 4-(nitromethyl)-1,3-dioxolane. Stage 2 transition state (TS2-H-M2) and 4-methylene-1,3-dioxolane product

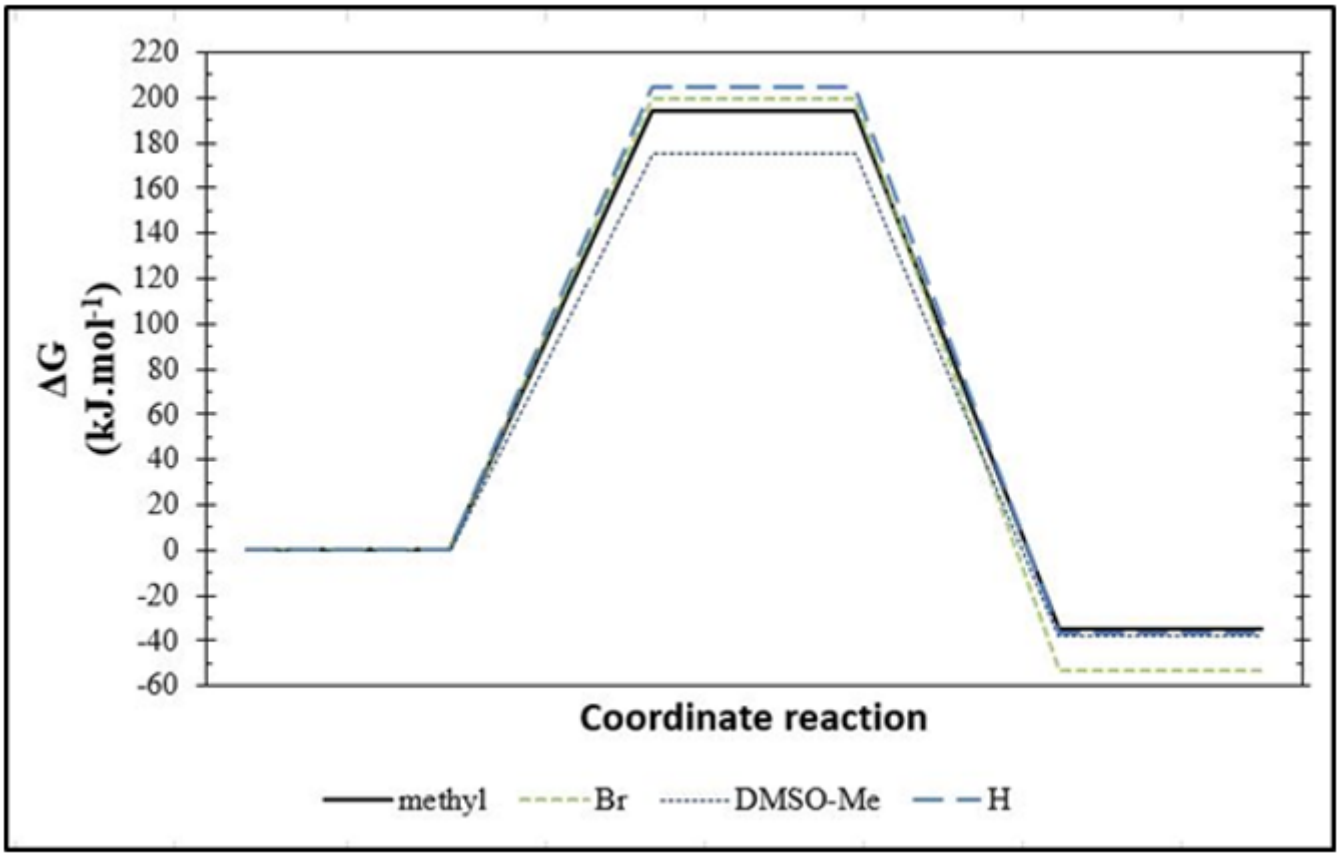

Figure 6

Gibbs energy profile for the decomposition reaction of 5-nitro-5-R-1,3-dioxane compounds. According to the computationally obtained data for R= H, methyl and Br